

Cobalt-Catalyzed C–H Activation and [3 + 2] Annulation with Allenes: Diastereoselective Synthesis of Indane Derivatives

Arnab Dey and Chandra M. R. Volla*



Cite This: *Org. Lett.* 2021, 23, 5018–5023



Read Online

ACCESS |



Metrics & More

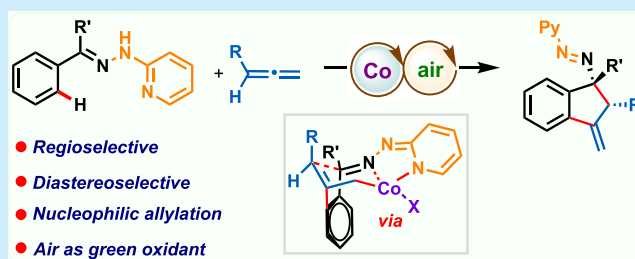


Article Recommendations



Supporting Information

ABSTRACT: An unprecedented bidentate directing-group-assisted cobalt-catalyzed oxidative C–H activation of aryl hydrazones followed by a *syn*-diastereoselective [3 + 2] annulation reaction has been achieved, employing allenes as the annulation partners. The selective 2,3-migratory insertion of allenes with arylcobalt(III) species and the subsequent intramolecular diastereoselective nucleophilic addition of η^1 -allylcobalt onto the imine resulted in [3 + 2] annulation over the alternative [4 + 2] annulation. Furthermore, the oxidative annulation obviates the need for stoichiometric metal oxidants and proceeds under aerobic conditions.



Transition-metal-catalyzed oxidative functionalization and annulation reactions of inert C–H bonds are emerging as one of the most appealing and powerful tools for the atom- and step-economic synthesis of heterocycles, drugs, and natural products.¹ This strategy has been dominated by rare and expensive noble transition-metal catalysts.² Capitalizing on this concept with more abundant and inexpensive first-row transition-metal catalysts has recently gained more interest.³ In this regard, earth-abundant cobalt(II) salts have attracted considerable attention for accomplishing oxidative C–H annulation reactions with different π -organic components such as alkenes, alkynes, and allenes.⁴ On a different note, the allylation of imines with allyl metal reagents is an efficient and straightforward method for accessing valuable homoallyl derivatives.⁵ Although the advantages of cobalt salts have been recognized in various organometallic reactions⁶ like hydrogenation, hydrofunctionalization, cross-coupling, and cycloaddition, their use in nucleophilic allylation reactions is surprisingly limited.⁷ As a result, the development of nucleophilic allylation reactions with η^1 -allylcobalt species is highly desired.

Allenes⁸ are versatile organic motifs with three reactive carbon centers, and they exhibit complex patterns of reactivity for migratory insertion based on electronic and steric factors.^{9,10} Unravelling these issues, various oxidative C–H annulation strategies with allenes, proceeding via Co- π -allyl intermediate **Int-A**, have been documented (Scheme 1a).¹¹ Although elegant, these oxidative transformations require stoichiometric amounts of transition-metal oxidants based on Mn(III) or Ag(I) for the regeneration of a cobalt catalyst, which inevitably limits the overall efficiency of the transformation. Therefore, extensive efforts have been devoted to exploring green and efficient oxidative transformations employ-

ing naturally abundant molecular oxygen or air as a terminal oxidant in cobalt catalysis.¹²

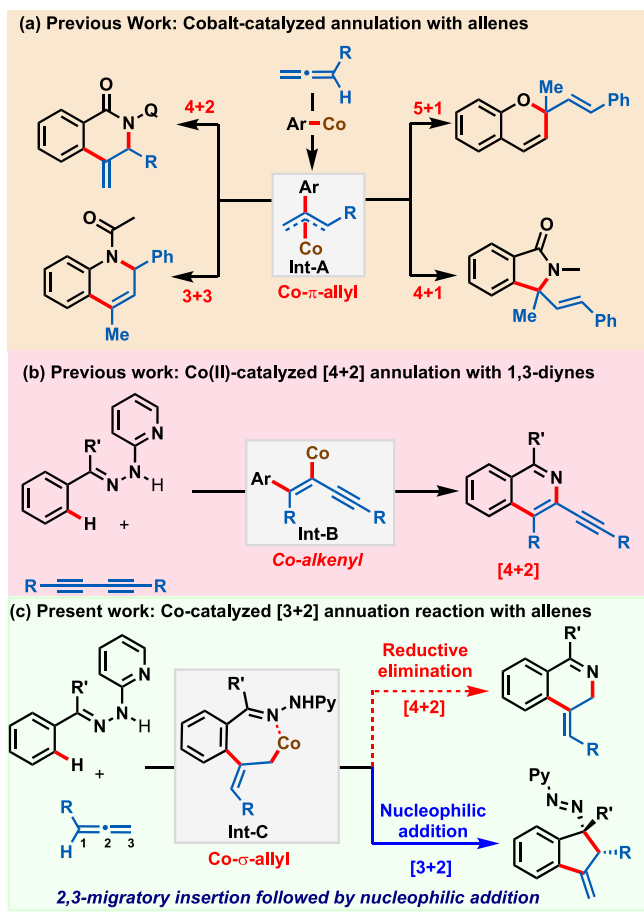
With our continuous interest in bidentate directing-group-assisted C–H activation,¹³ we recently reported a Co(II)-catalyzed [4 + 2] annulation reaction with 1,3-diyne.¹⁴ The reaction ensues via a key Co-alkenyl intermediate **Int-B** under redox-neutral conditions with the N–N bond acting as an internal oxidant (Scheme 1b). To expand the synthetic repertoire of allenes, we envisioned a 2-hydrazinepyridine-assisted annulation reaction of allenes with Co(II) salts (Scheme 1c). The outcome of this anticipated strategy relies on two independent competitive pathways: (1) Reductive elimination followed by N–N bond cleavage (analogous to 1,3-diyne) can produce [4 + 2] annulated isoquinoline derivatives, or (2) a nucleophilic attack onto the imine can afford [3 + 2] annulated indane derivatives. On the basis of this hypothesis, the reaction between hydrazone derivatives and allenes was studied in the presence of Co(II) salts, and to our delight, a preferential nucleophilic attack on the imine was observed, furnishing indane derivatives having two new stereogenic centers with high *syn* diastereoselectivity for the aryl and azo groups.¹⁵ The observed high stereocontrol in the [3 + 2] annulation is a manifestation of the highly selective 2,3-migratory insertion of allene with the organocobalt(III) species, leading to Co- σ -allyl intermediate **Int-C**. Furthermore,

Received: May 5, 2021

Published: June 16, 2021

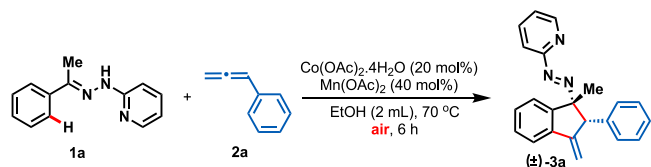


Scheme 1. Overview of the Work



the divergent reactivity observed between **Int-B** (Co-alkenyl) and **Int-C** (Co- σ -allyl) is the main highlight, and it can be ascertained to the higher nucleophilicity of the Co- σ -allyl species. It is worth mentioning that the cobalt catalyst was regenerated using air as the green oxidant.

We commenced our studies with hydrazone **1a** and phenylallene **2a** as the model substrates. After rigorous optimization of various reaction parameters, we arrived at the following optimized conditions: 20 mol % $\text{Co}(\text{OAc})_2 \cdot 4\text{H}_2\text{O}$ and 40 mol % $\text{Mn}(\text{OAc})_2$ at 70 °C in EtOH under an air atmosphere to observe 83% of the desired [3 + 2] annulation product **3a** (isolated yield of 78%) (Table 1, entry 1).¹⁵ The ¹H NMR of the crude reaction mixture indicated the formation of a single diastereomer, and the *syn* configuration of the phenyl moiety and the azo group in the product **3a** were confirmed by a nuclear Overhauser effect (NOE) study and single-crystal X-ray diffraction analysis of **3a**. Lowering the loading of $\text{Mn}(\text{OAc})_2$ resulted in lower yields, and **3a** was observed in only 10% yield in the absence of $\text{Mn}(\text{OAc})_2$ (entries 2 and 3). Whereas, additives like NaOAc or NaOPiv instead of $\text{Mn}(\text{OAc})_2$ produced **3a** in inferior yields (entries 4 and 5), the use of $\text{Cu}(\text{OAc})_2$ or PivOH was found to be deleterious (entries 6 and 7). Other Co(II) salts did not show much improvement, as **3a** was observed in 18–35% yield (entries 8–11). The screening of various polar protic and nonprotic solvents indicated the crucial role of EtOH as a solvent for the success of the reaction (entry 12). The temperature is found to be optimum at 70 °C, as no reaction was observed at room temperature, and the yield of **3a**

Table 1. Optimization of Reaction Conditions^a

entry	variation from standard conditions	yield (%) ^b
1	none	83 (78) ^c
2	20 mol % $\text{Mn}(\text{OAc})_2$	50
3	without $\text{Mn}(\text{OAc})_2$	10
4	NaOAc instead of $\text{Mn}(\text{OAc})_2$	25
5 ^d	NaOPiv instead of $\text{Mn}(\text{OAc})_2$	40 ^c
6 ^d	$\text{Cu}(\text{OAc})_2$ instead of $\text{Mn}(\text{OAc})_2$	
7 ^d	PivOH instead of $\text{Mn}(\text{OAc})_2$	
8 ^d	with $\text{CoCl}_2 \cdot 6\text{H}_2\text{O}$	20
9 ^e	with $\text{Co}(\text{acac})_2$	35
10 ^e	with $\text{Co}(\text{NO}_3)_2 \cdot 6\text{H}_2\text{O}$	18
11 ^e	with $\text{CoSO}_4 \cdot 7\text{H}_2\text{O}$	19
12 ^e	HFIP, TFE, <i>t</i> -BuOH, MeOH, DCE, CH_3CN , acetone	<25%
13	at room temperature	
14	at 100 °C	72
15	without $\text{Co}(\text{OAc})_2 \cdot 4\text{H}_2\text{O}$	

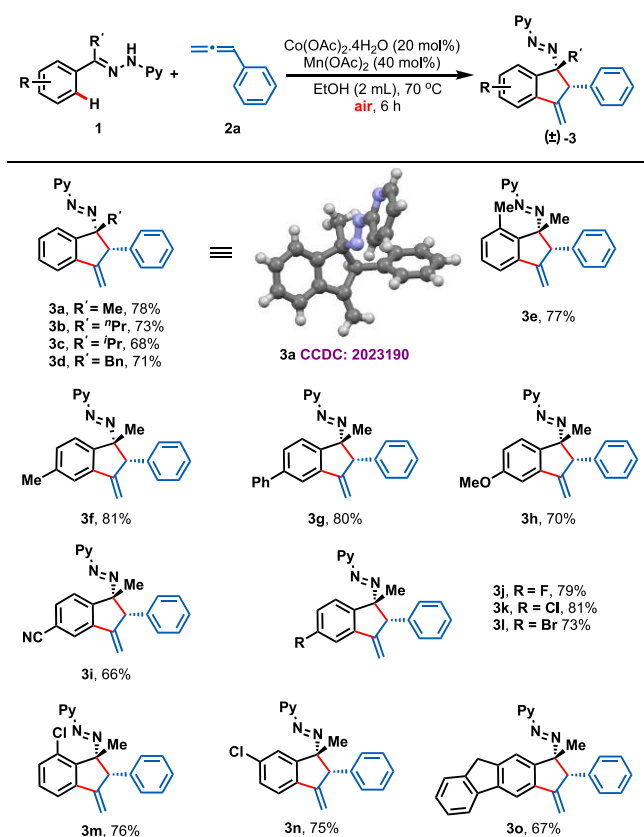
^aReaction conditions: **1a** (0.2 mmol), **2a** (0.6 mmol), $\text{Co}(\text{OAc})_2 \cdot 4\text{H}_2\text{O}$ (20 mol %), $\text{Mn}(\text{OAc})_2$ (40 mol %), EtOH (2 mL) at 70 °C for 6 h. ^bYield is calculated based on ¹H NMR of the crude reaction mixture using 1,3,5-trimethoxybenzene as an internal standard. ^cYield refers to isolated yield after column chromatography. ^d20 mol % additive was used. ^eUsing 20 mol % NaOPiv.

dropped to 72% at 100 °C (entries 13 and 14). As expected, no product was detected in the absence of cobalt salt (entry 15).

With the optimized reaction conditions in hand, we started to explore the substrate scope of our methodology by treating a variety of substituted hydrazone derivatives **1** with phenyl allene **2a** (Table 2). We were pleased to see the formation of the indane derivatives **3a–3o** in moderate to good yields with diversely substituted hydrazone derivatives **1**, irrespective of the electronic and steric nature of the substituents. Both electron-donating and electron-withdrawing substituents were compatible under the optimized reactions. Interestingly, *meta*-chloro-substituted hydrazone **1n** and 2-fluorenyl hydrazone **1o** afforded the corresponding products by selective activation of the less sterically hindered C–H bond (**3n** and **3o** in 75 and 67% yield, respectively).

To further investigate the generality and scope of the methodology, several allenes **2** were tested with hydrazone **1a**. As evident from Table 3, various substituents on the arylallene were compatible to deliver the indane derivatives **3p–3ad** in 53–95% yield. The structure and stereochemistry of indanes were further confirmed by the X-ray crystallography analysis of **3w**. The 2-naphthyl-substituted allene **2m** produced the corresponding product **3ab** in an excellent yield of 95%. Captivatingly, disubstituted allenes **2n** and **2o** reacted smoothly under the standard conditions to provide the indanes **3ac** and **3ad** in 53 and 59% yield, respectively, with the selective formation of the *E*-isomer, as confirmed by NOE analysis.¹⁵ The preferential formation of the *E*-isomer is consistent with the proposed 2,3-migratory insertion of allene with the arylcobalt(III) species, leading to the Co- σ -allyl complex **Int C**. We subsequently evaluated the amenability of

Table 2. Substrate Scope with Different Hydrazone Derivatives

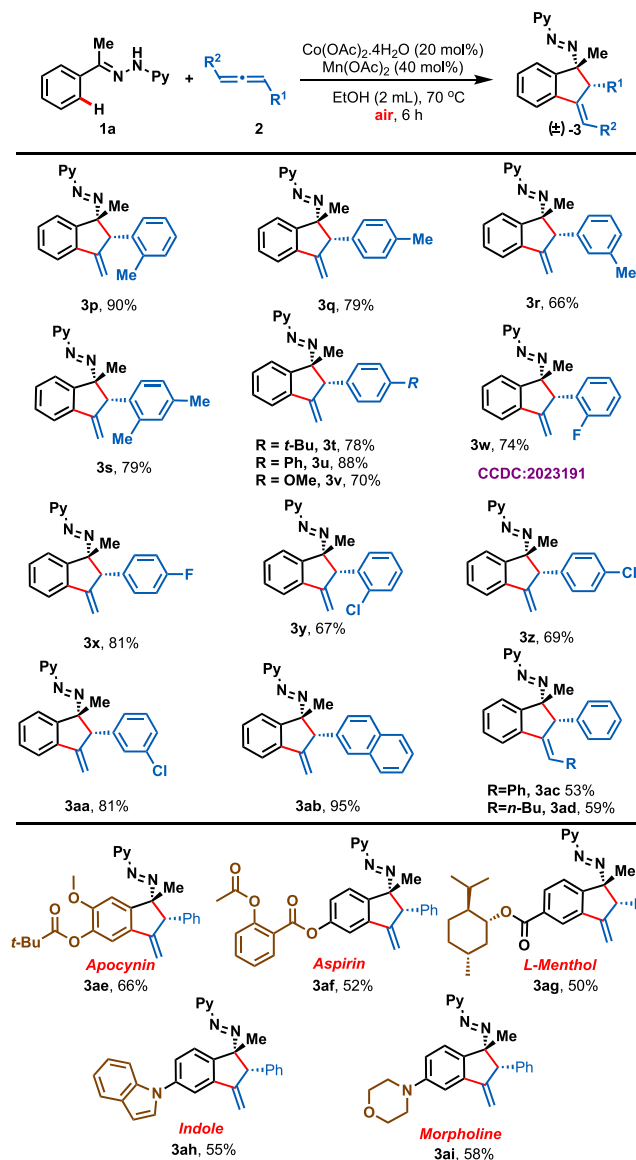


this approach for the late-stage modification of biologically relevant hydrazone derivatives. When an apocynin-derived hydrazone derivative was subjected to this protocol, the target product 3ae was isolated in 66% yield. Similarly, other bioactive molecules like aspirin-, L-menthol-, indole-, and morpholine-substituted hydrazones also smoothly underwent the annulation to afford the corresponding functionalized indane derivatives 3af–3ai in 50–58% yield.

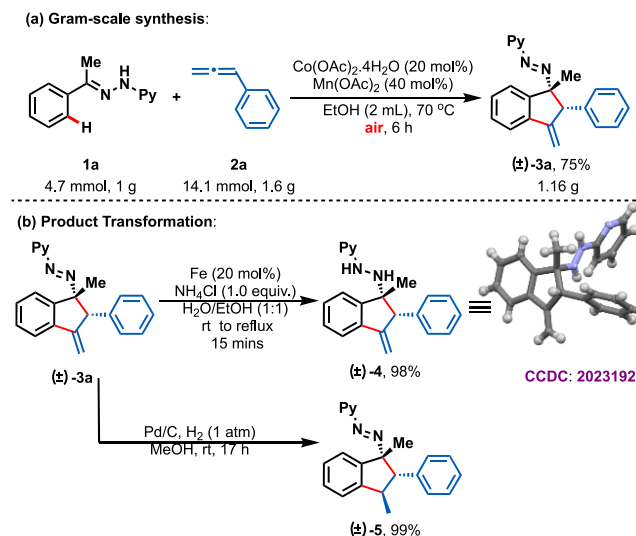
A gram-scale reaction was conducted (Scheme 2) by reacting 1.0 g of 1a and 1.6 g of 2a, and we were pleased to observe the formation of 1.16 g of indane 3a (75% yield). To further expand the synthetic utility, we performed selective reduction reactions on 3a. Reduction using Fe powder (20 mol%) and NH₄Cl (1 equiv) specifically reduced the azo group to hydrazine functionality and provided 4 in 98% isolated yield. Under Pd-catalyzed hydrogenation with 1 atm of H₂, the exo-methylene moiety was selectively reduced to generate 5 in quantitative yield as a single diastereomer (Scheme 2b).

To get more insights into the reaction mechanism, various control, competitive, and deuterium labeling experiments were performed, as shown in Scheme 3. Under the optimized conditions, the control reaction between *N*-phenyl hydrazone 6 and 2a did not provide any indane product, indicating the importance of bidentate pyridine coordination with the cobalt catalyst (Scheme 3a). Another control experiment was conducted by using *N*-methyl hydrazone 7 instead of 1, and no product was detected in this case either, suggesting that an initial N–Co bond formation is crucial for C–H bond activation (Scheme 3a). The exchange experiments on 1a and [D]₅-1a either with allene or without the allene implied no H/D exchange or D/H exchange (see the Supporting

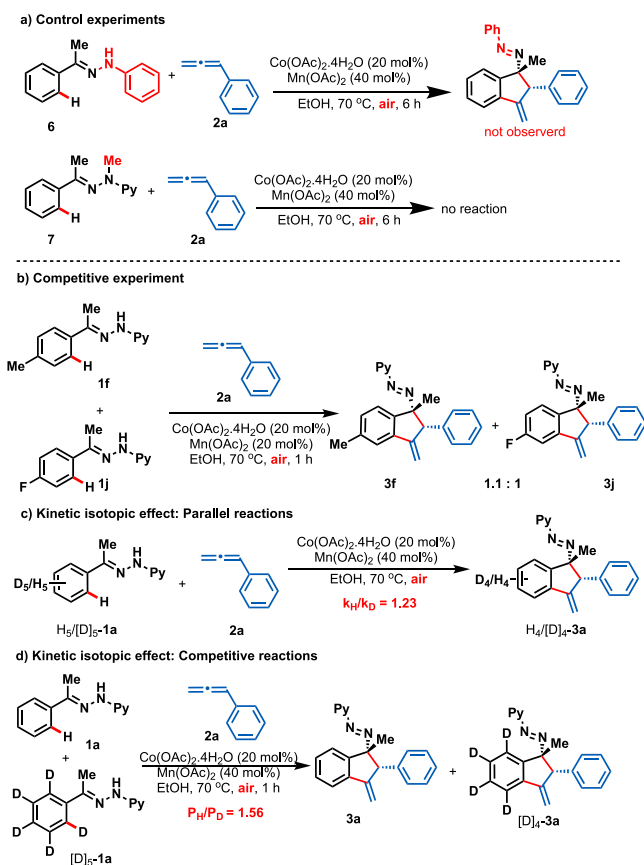
Table 3. Substrate Scope with Different Allenes



Scheme 2. Scale-up Reaction and Product Transformations



Scheme 3. Preliminary Mechanistic Investigation

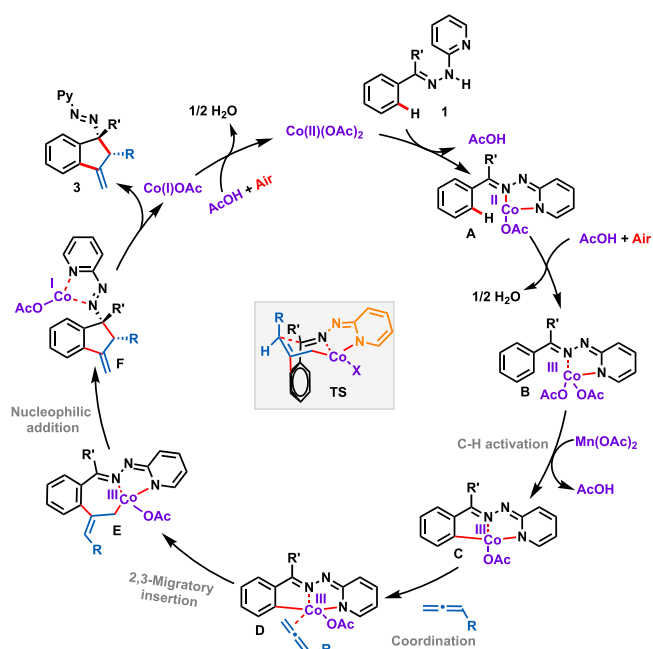


Information). When a 1:1 mixture of 4-Me **1f**- and 4-F **1j**-substituted hydrazone derivatives was reacted under our standard conditions with **2a**, a 1.1:1 mixture of **3f** and **3j** was obtained, suggesting that electrophilic cobaltation is unlikely (Scheme 3b). Parallel kinetic studies with **1a** and $[D]_5\text{-1a}$ afforded a kinetic isotope effect value (k_H/k_D) of 1.23 (Scheme 3c) and a competitive isotopic effect between **1a** and $[D]_5\text{-1a}$ produced a product distribution value of (P_H/P_D) 1.56 (Scheme 3d). These combined studies suggest that C–H cobaltation is irreversible and might not be the rate-limiting step.

On the basis of the preliminary mechanistic studies and literature precedence,^{12b,16} a plausible reaction mechanism has been proposed, as shown in Scheme 4. The catalytic cycle is initiated by the interaction of hydrazone derivative **1** with the Co(II) catalyst to generate intermediate **A**. Intermediate **A**, after aerial oxidation followed by a Mn(OAc)₂-assisted (acting as a base) concerted metalation deprotonation (CMD) process, leads to the C–H metalated complex **C**. The subsequent coordination of the allene and selective 2,3-migratory insertion of the less-substituted double bond lead to the allyl cobalt intermediate **E** (σ -allyl complex).¹⁵ The intramolecular nucleophilic addition of the allylcobalt species onto the imine carbon proceeds via a six-membered cyclic transition state **TS** followed by elimination, furnishing the Co(I) intermediate **F**. Decomplexation gives the product **3** and Co(I), which, after aerial oxidation, regenerates the active Co(II) catalyst.

In conclusion, we have demonstrated a bidentate directing-group-assisted oxidative C–H activation and a *syn*-diastereoselective [3 + 2] annulation strategy of hydrazones with

Scheme 4. Proposed Reaction Mechanism



allenes to access indane derivatives using simple and commercially available cobalt(II) salts. Various allenes reacted smoothly with diversely substituted hydrazones irrespective of the steric and electronic nature of the substituents. The *syn* configuration of the product was confirmed by a NOE study and X-ray diffraction analysis. The use of simple cobalt(II) salts and air as the greener oxidant makes the transformation more valuable and appealing. Furthermore, the protocol was compatible with the functionalization of biologically relevant hydrazones.

■ ASSOCIATED CONTENT

Supporting Information

The Supporting Information is available free of charge at <https://pubs.acs.org/doi/10.1021/acs.orglett.1c01521>.

Additional experimental procedures and X-ray crystallographic analysis (PDF)

Accession Codes

CCDC 2023190–2023192 contain the supplementary crystallographic data for this paper. These data can be obtained free of charge via www.ccdc.cam.ac.uk/data_request/cif, or by emailing data_request@ccdc.cam.ac.uk, or by contacting The Cambridge Crystallographic Data Centre, 12 Union Road, Cambridge CB2 1EZ, UK; fax: +44 1223 336033.

■ AUTHOR INFORMATION

Corresponding Author

Chandra M. R. Volla – Department of Chemistry, Indian Institute of Technology Bombay, Mumbai 400076, India; orcid.org/0000-0002-8497-1538; Email: chandra.volla@chem.iitb.ac.in

Author

Arnab Dey – Department of Chemistry, Indian Institute of Technology Bombay, Mumbai 400076, India; orcid.org/0000-0001-6176-8775

Complete contact information is available at:
<https://pubs.acs.org/10.1021/acs.orglett.1c01521>

Notes

The authors declare no competing financial interest.

ACKNOWLEDGMENTS

We are grateful to SERB, India for supporting this activity (CRG/2019/005059). We also thank Mr. Darshan Mhatre, IIT Bombay for the single-crystal X-ray diffraction analysis.

REFERENCES

- (1) (a) Dalton, T.; Faber, T.; Glorius, F. C-H Activation: Toward Sustainability and Applications. *ACS Cent. Sci.* **2021**, *7*, 245–261. (b) Khake, S. M.; Chatani, N. Nickel-Catalyzed C-H Functionalization Using A Non-directed Strategy. *Chem.* **2020**, *6*, 1056–1081. (c) Rej, S.; Ano, Y.; Chatani, N. Bidentate Directing Groups: An Efficient Tool in C-H Bond Functionalization Chemistry for the Expedient Construction of C-C Bonds. *Chem. Rev.* **2020**, *120*, 1788–1887.
- (2) (a) He, C.; Whitehurst, W. G.; Gaunt, M. J. Palladium-Catalyzed C(sp³)-H Bond Functionalization of Aliphatic Amines. *Chem.* **2019**, *5*, 1031–1058. (b) Rej, S.; Chatani, N. Rhodium-Catalyzed C(sp²)- or C(sp³)-H Bond Functionalization Assisted by Removable Directing Groups. *Angew. Chem., Int. Ed.* **2019**, *58*, 8304–8329.
- (3) (a) Loup, J.; Dhawa, U.; Pesciaoli, F.; Wencel-Delord, J.; Ackermann, L. Enantioselective C-H Activation with Earth-Abundant 3d Transition Metals. *Angew. Chem., Int. Ed.* **2019**, *58*, 12803–12818. (b) Gandeepan, P.; Muller, T.; Zell, D.; Cera, G.; Warratz, S.; Ackermann, L. 3d Transition Metals for C-H Activation. *Chem. Rev.* **2019**, *119*, 2192–2452.
- (4) (a) Moselage, M.; Li, J.; Ackermann, L. Cobalt-Catalyzed C-H Activation. *ACS Catal.* **2016**, *6*, 498–525. (b) Prakash, S.; Kuppusamy, R.; Cheng, C.-H. Cobalt(II)-catalyzed C-H functionalization using an N,N'-bidentate directing group. *ChemCatChem* **2018**, *10*, 683–705. (c) Baccalini, A.; Vergura, S.; Dolui, P.; Zanon, G.; Maiti, D. Recent advances in cobalt-catalyzed C-H functionalizations. *Org. Biomol. Chem.* **2019**, *17*, 10119–10141. (d) Mei, R.; Dhawa, U.; Samanta, R. C.; Ma, W.; Wencel-Delord, J.; Ackermann, L. Cobalt-Catalyzed Oxidative C-H Activation: Strategies and Concepts. *ChemSusChem* **2020**, *13*, 3306–3356.
- (5) (a) Yus, M.; González-Gómez, J. C.; Foubelo, F. Catalytic Enantioselective Allylation of Carbonyl Compounds and Imines. *Chem. Rev.* **2011**, *111*, 7774–7854. (b) Denmark, S. E.; Fu, J. Catalytic Enantioselective Addition of Allylic Organometallic Reagents to Aldehydes and Ketones. *Chem. Rev.* **2003**, *103*, 2763–2794.
- (6) Hapke, M.; Hilt, G. *Cobalt Catalysis in Organic Synthesis*; Wiley-VCH Verlag GmbH & Co. KGaA, 2020.
- (7) (a) Han, J.-F.; Guo, P.; Zhang, X.-G.; Liao, J.-B.; Ye, K.-Y. Recent advances in cobalt-catalyzed allylic functionalization. *Org. Biomol. Chem.* **2020**, *18*, 7740–7750. (b) Michigami, K.; Mita, T.; Sato, Y. Cobalt-Catalyzed Allylic C(sp³)-H Carboxylation with CO₂. *J. Am. Chem. Soc.* **2017**, *139*, 6094–6097. (c) Mita, T.; Hanagata, S.; Michigami, K.; Sato, Y. Co-Catalyzed Direct Addition of Allylic C(sp³)-H Bonds to Ketones. *Org. Lett.* **2017**, *19*, 5876–5879. (d) Boerth, J. A.; Maity, S.; Williams, S. K.; Mercado, B. Q.; Ellman, J. A. Selective and synergistic cobalt(III)-catalyzed three-component C-H bond addition to dienes and aldehydes. *Nat. Catal.* **2018**, *1*, 673–679. (e) Wu, L.; Shao, Q.; Yang, G.; Zhang, W. Cobalt-Catalyzed Asymmetric Allylation of Cyclic Ketimines. *Chem. - Eur. J.* **2018**, *24*, 1241–1245.
- (8) For selected reviews, see: (a) Zimmer, R.; Dinesh, C. U.; Nandan, E.; Khan, F. A. Palladium-Catalyzed Reactions of Allenes. *Chem. Rev.* **2000**, *100*, 3067–3125. (b) Ma, S. Palladium-Catalyzed Reactions of Allenes. *Chem. Rev.* **2005**, *105*, 2829–2871. (c) Hashmi, A. S. K. New and Selective Transition Metal Catalyzed Reactions of Allenes. *Angew. Chem., Int. Ed.* **2000**, *39*, 3590–3593.
- (9) For reviews on allenes in C-H activation, see: (a) Santhoshkumar, R.; Cheng, C.-H. Fickle Reactivity of Allenes in Transition-Metal-Catalyzed C-H Functionalizations. *Asian J. Org. Chem.* **2018**, *7*, 1151–1163. (b) Shukla, R. K.; Nair, A. M.; Volla, C. M. R. Allenes: Versatile Building Blocks in Cobalt-Catalyzed C-H Activation. *Synlett* **2021**, DOI: 10.1055/a-1471-7307.
- (10) For selected references, see: (a) Zeng, R.; Fu, C.; Ma, S. Highly Selective Mild Stepwise Allylation of N-Methoxybenzamides with Allenes. *J. Am. Chem. Soc.* **2012**, *134*, 9597–9600. (b) Wang, H.; Glorius, F. Mild Rhodium(III)-Catalyzed CCH Activation and Intermolecular Annulation with Allenes. *Angew. Chem., Int. Ed.* **2012**, *51*, 7318–7322. (c) Nakanowatari, S.; Müller, T.; Oliveira, J. C. A.; Ackermann, L. Bifurcated Nickel-Catalyzed Functionalizations: Heteroarene C-H Activation with Allenes. *Angew. Chem., Int. Ed.* **2017**, *56*, 15891–15895. (d) Casanova, N.; Del Rio, K. P.; García-Fandiño, R.; Mascareñas, J. L.; Gullías, M. Palladium(II)-Catalyzed Annulation between *ortho*-Alkenylphenols and Allenes. Key Role of the Metal Geometry in Determining the Reaction Outcome. *ACS Catal.* **2016**, *6*, 3349–3353. (e) Wang, C.; Wang, A.; Rueping, M. Manganese-Catalyzed C-H Functionalizations: Hydroarylations and Alkenylations Involving an Unexpected Heteroaryl Shift. *Angew. Chem., Int. Ed.* **2017**, *56*, 9935–9938. (f) Kuninobu, Y.; Yu, P.; Takai, K. Rhenium-Catalyzed Diastereoselective Synthesis of Aminoindanes via the Insertion of Allenes into a C-H Bond. *Org. Lett.* **2010**, *12*, 4274–4276. (g) Tran, D. N.; Cramer, N. *syn*-Selective Rhodium(I)-Catalyzed Allylations of Ketimines Proceeding through a Directed C-H Activation/Allene Addition Sequence. *Angew. Chem., Int. Ed.* **2010**, *49*, 8181–8184. (h) Tran, D. N.; Cramer, N. Rhodium Catalyzed Dynamic Kinetic Asymmetric Transformations of Racemic Allenes by the [3 + 2] Annulation of Aryl Ketimines. *Angew. Chem., Int. Ed.* **2013**, *52*, 10630–10634. (i) Zhai, S.; Qiu, S.; Chen, X.; Tao, C.; Li, Y.; Cheng, B.; Wang, H.; Zhai, H. Trifunctionalization of Allenes via Cobalt-Catalyzed MHP-Assisted C-H Bond Functionalization and Molecular Oxygen Activation. *ACS Catal.* **2018**, *8*, 6645–6649. (j) Shukla, R. K.; Nair, A. M.; Khan, S.; Volla, C. M. R. Cobalt-Catalyzed C8-Dienylation of Quinoline-N-Oxides. *Angew. Chem., Int. Ed.* **2020**, *59*, 17042–17048.
- (11) (a) Thrimurtulu, N.; Dey, A.; Maiti, D.; Volla, C. M. R. Cobalt-Catalyzed sp²-C-H Activation: Intermolecular Heterocyclization with Allenes at Room Temperature. *Angew. Chem., Int. Ed.* **2016**, *55*, 12361–12365. (b) Kuppusamy, R.; Muralirajan, K.; Cheng, C.-H. Cobalt(III)-Catalyzed [5 + 1] Annulation for 2H-Chromenes Synthesis via Vinylic C-H Activation and Intramolecular Nucleophilic Addition. *ACS Catal.* **2016**, *6*, 3909–3913. (c) Kuppusamy, R.; Santhoshkumar, R.; Boobalan, R.; Wu, H. R.; Cheng, C.-H. Synthesis of 1,2-Dihydroquinolines by Co(III)-Catalyzed [3 + 3] Annulation of Anilides with Benzylallenes. *ACS Catal.* **2018**, *8*, 1880–1883. (d) Boobalan, R.; Santhoshkumar, R.; Cheng, C.-H. Co(III)-Catalyzed [4 + 1] Annulation of Amides with Allenes via C-H Activation. *Adv. Synth. Catal.* **2019**, *361*, 1140–1145. (e) Boobalan, R.; Kuppusamy, R.; Santhoshkumar, R.; Gandeepan, P.; Cheng, C.-H. Access to Isoquinolin-1(2H)-ones and Pyridones by Cobalt-Catalyzed Oxidative Annulation of Amides with Allenes. *ChemCatChem* **2017**, *9*, 273–277. (f) Lan, T.; Wang, L.; Rao, Y. Regioselective Annulation of Aryl Sulfonamides with Allenes through Cobalt-Promoted C-H Functionalization. *Org. Lett.* **2017**, *19*, 972–975.
- (12) (a) Mei, R.; Wang, H.; Warratz, S.; Macgregor, S. A.; Ackermann, L. Cobalt-Catalyzed Oxidative C-H/N-H Alkyne Annulation: Mechanistic Insights and Access to Anticancer Agents. *Chem. - Eur. J.* **2016**, *22*, 6759–6763. (b) Martínez, Á. M.; Rodríguez, N.; Gómez-Arrayás, R.; Carretero, J. C. Cobalt-Catalyzed *ortho*-C-H Functionalization/Alkyne Annulation of Benzylamine Derivatives: Access to Dihydroisoquinolines. *Chem. - Eur. J.* **2017**, *23*, 11669–11676.
- (13) (a) Thrimurtulu, N.; Nallagonda, R.; Volla, C. M. R. Cobalt-catalyzed aryl C-H activation and highly regioselective intermolecular annulation of sulfonamides with allenes. *Chem. Commun.* **2017**, *53*,

1872–1875. (b) Nallagonda, R.; Thrimurtulu, N.; Volla, C. M. R. Cobalt-Catalyzed Diastereoselective [4 + 2] Annulation of Phosphinamides with Heterobicyclic Alkenes at Room Temperature. *Adv. Synth. Catal.* **2018**, *360*, 255–260. (c) Dey, A.; Thrimurtulu, N.; Volla, C. M. R. Cobalt-Catalyzed Annulation Reactions of Alkylidenecyclopropanes: Access to Spirocyclopropanes at Room Temperature. *Org. Lett.* **2019**, *21*, 3871–3875.

(14) Dey, A.; Volla, C. M. R. Traceless Bidentate Directing Group Assisted Cobalt-Catalyzed sp^2 -C-H Activation and [4 + 2]-Annulation Reaction with 1,3-Diynes. *Org. Lett.* **2020**, *22*, 7480–7485.

(15) See the [Supporting Information](#) for a schematic representation and more optimization details.

(16) Planas, O.; Whiteoak, C. J.; Martin-Diaconescu, V.; Gamba, I.; Luis, J. M.; Parella, T.; Company, A.; Ribas, X. Isolation of Key Organometallic Aryl-Co(III) Intermediates in Cobalt-Catalyzed C(sp^2)-H Functionalizations and New Insights into Alkyne Annulation Reaction Mechanisms. *J. Am. Chem. Soc.* **2016**, *138*, 14388–14397.